



## Research article

# Recycling industrial waste polymer as a binder system for ceramic injection molding feedstock

Daniel Sanetnik<sup>\*</sup>, Tomas Sedlacek

Centre of Polymer Systems, University Institute, Tomas Bata University in Zlin, Trida T. Bati 5678, 760 01, Zlin, Czech Republic



## ARTICLE INFO

## Keywords:

Industrial waste binder system  
Recycling polymer  
Highly filled polymer  
Ceramic injection molding

## ABSTRACT

Ceramic injection molding is a widely used manufacturing process for producing high-precision ceramic components. However, the high cost of traditional binder systems, as well as non-ecological aspects of these binders, may limit its broader applications. This study investigates the potential use of polyvinyl butyral industrial waste containing plasticizer as a sustainable alternative binder system for ceramic injection molding, utilizing alumina powder with a mean particle size of 0.7  $\mu\text{m}$ . The mixing behavior of the binder-powder mixture was evaluated through torque measurements, identifying a critical solid loading point at 56 vol%. The rheological properties of the feedstocks were characterized, revealing that their viscosity remained below the recommended threshold of 1000 Pa s, suitable for ceramic injection molding. The activation energy, ranging from 18 kJ/mol to 45 kJ/mol, demonstrated favorable temperature sensitivity for the process. Subsequently, the feedstocks were successfully injection molded into test specimens, followed by the debinding and sintering processes to achieve the final density. Mechanical testing of the sintered ceramic parts indicated performance comparable to parts produced with traditional binder systems, with final densities exceeding 4 g/cm<sup>3</sup>, a bending modulus of approximately 15000 N/mm<sup>2</sup>, and bending strength up to 139 N/mm<sup>2</sup>. These findings suggest that incorporating industrial waste polymer as a binder system is a cost-effective, environmentally friendly alternative that maintains the quality of molded ceramic parts.

## 1. Introduction

In the past few decades, the utilization of highly filled polymers with ceramic particles (40–50 vol %) has emerged as a promising material for the economical and complex production of products with precise tolerances using the ceramic injection molding technology (CIM), e.g. the process finds its applications in various industries such as aerospace, defense, biomedical, automotive, electronics, and consumer goods. The Ceramic Injection Molding (CIM) process involves four essential steps commonly used in manufacturing (Fig. 1). The first step is feedstock preparation, where ceramic powder is mixed with a binder, such as wax or a thermoplastic polymer. This binder helps hold the ceramic particles together, creating a mixture with the right consistency for molding. Next, in the injection molding phase, the prepared feedstock is injected into a mold cavity under high pressure using a screw or plunger. The mold, typically made from steel or aluminum, is designed to shape the ceramic into the desired form, allowing for precise and accurate production of complex shapes. Following molding, the debinding step occurs. Here, the molded part is heated to remove the binder material. This process takes place in two stages: first, the part is heated to a temperature where the binder vaporizes,

<sup>\*</sup> Corresponding author.

E-mail address: [dsanetnik@utb.cz](mailto:dsanetnik@utb.cz) (D. Sanetnik).

<https://doi.org/10.1016/j.heliyon.2024.e39610>

Received 8 July 2024; Received in revised form 24 September 2024; Accepted 18 October 2024

Available online 19 October 2024

2405-8440/© 2024 The Authors. Published by Elsevier Ltd. This is an open access article under the CC BY-NC license (<http://creativecommons.org/licenses/by-nc/4.0/>).

leaving behind a porous ceramic green body. In the second stage, the green body is heated further to remove any remaining binder and initiate pre-sintering of the ceramic particles. Finally, the sintering step involves heating the green body to a high temperature, usually above 1200 °C, in a furnace. This causes the ceramic particles to bond together, forming a dense, solid ceramic part. Sintering is crucial for achieving the desired mechanical and physical properties of the final ceramic product.

The feedstock preparation is a critical issue as the choice of polymer binder system affects the entire process. Therefore, the polymer binder system plays a crucial role in the CIM process, as it must not only adhere well to the ceramic powder but also impart suitable rheological and mechanical properties to the feedstock. A well-designed binder system should facilitate the formation of a homogeneous mixture of the ceramic powder and polymer binder, which is critical for achieving the desired product quality. The successful use of polymer binder systems in CIM technology is largely dependent on their ability to form a stable feedstock with high solids loading, low viscosity, and good rheological properties, while also exhibiting good green strength and thermal stability during the debinding and sintering stages. As a result, at least two-component polymer binder systems are usually employed, where each component serves a specific purpose [1,2].

The main component of the binder system, typically a low molecular weight polymer, ensures the flow properties of the feedstock. Moballeghe [3] utilized a binder system based on paraffin wax, which exhibited desirable behavior during injection molding, debinding, and sintering. Other studies [4] have focused on developing wax-based binder systems filled with cubic yttria-stabilized zirconia particles to achieve high-density and homogeneous microstructures after sintering. However, it has been reported by Thomas-Vielma [5] that a high content of paraffin wax in the binder system could lead to poor shape retention of the component during the initial stage of debinding. Therefore, it is more promising to use semi-crystalline waxes, such as carnauba wax (CW) or acrawax (AW) [6]. The use of these waxes has also been found to increase the efficiency of the process in terms of energy, time, and consumption of chemicals and media [7].

The second component of the binder system is a high molecular weight polymer, also known as the backbone polymer, which provides strength to the initial stages of sintering. Traditionally, low-density polyethylene (LDPE) or high-density polyethylene (HDPE) are used due to their appropriate properties during the injection molding stage [8]. Recent studies [9] have shown that a binder system comprising of both LDPE and HDPE can result in increased tensile, impact, and bending properties of samples after debinding. Specifically, the addition of 6 wt% LDPE to the binder system has been found to improve the aforementioned properties by 20 %. Alternatively, the ethylene-vinyl acetate (EVA) copolymer has also been proposed as a potential backbone component of the binder system [10].

Currently, environmental concerns and non-toxicity have gained significant attention in the field of binder systems, leading many researchers to investigate the potential of partially water-soluble systems based on polyethylene glycol (PEG) [11–13] that is usually combined with backbone polymers such as polymethyl methacrylate (PMMA) [14,15] or polyvinyl butyral (PVB) [16]. The growing interest in PVB as a binder system is primarily due to its ability to blend with other homopolymers, which results from the intra-chain repulsion between different units within the copolymer, and its insolubility in water [17,18]. Due to strong intramolecular interactions among its macromolecular chains, PVB exhibits relatively higher viscosity. Despite this, PVB allows for efficient powder wetting and provides a consistent feedstock. It effectively keeps the powder particles in position and preserves the shape of the material during the debinding stage [17]. This characteristic enables PVB to provide the required performance in terms of processing feedstock and sample strength prior to sintering. However, the use of virgin polymers in binder systems is still not considered an environmentally friendly process in current studies.

Therefore, to address the increasing concerns about environmental sustainability and waste reduction, our study aimed to explore the potential of using industrial waste polymers as binder systems for ceramic injection molding. Specifically, we investigated the feasibility of employing PVB industrial waste, which contains plasticizer, as a binder material. The presence of plasticizer is expected to ensure appropriate viscosity during the injection molding process, eliminating the need for additional components or additives. We hypothesized that PVB with plasticizer would provide effective adhesion to ceramic particles while delivering the required mechanical properties and desirable rheological behavior. In conclusion, the findings of this study could have significant implications for the sustainable production of ceramic parts and the reduction of waste associated with plastic disposal, while also reducing the cost of production. The proposed use of industrial waste polymer as a binder system, and in particular, the use of PVB containing plasticizer, presents a promising direction for future research in this area.

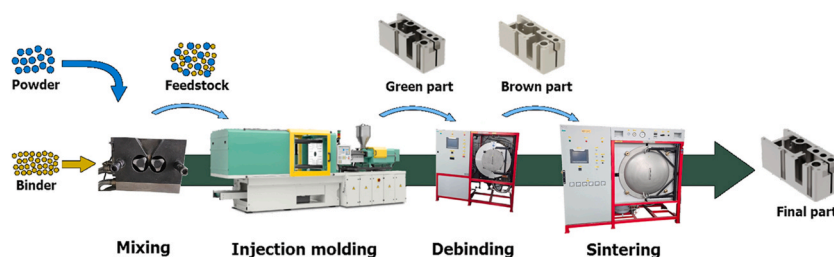


Fig. 1. Processing steps in powder injection molding technology.

## 2. Experimental

### 2.1. Materials

The powder used in this study was aluminum oxide ( $\text{Al}_2\text{O}_3$ ) MARTOXID MR70, supplied by ALBEMARLE Corporation (Germany). It has a particle size distribution ranging from D10: 0.1–0.4  $\mu\text{m}$ , D50: 0.5–0.8  $\mu\text{m}$ , to D90: 1.5–3.0  $\mu\text{m}$ , as specified in the supplier's datasheet. The precise particle size distribution was measured using a laser diffraction particle size analyzer Malvern Mastersizer 3000 (UK). The results of the particle size analysis are summarized in Fig. 2. Accurate characterization of the particle size distribution of aluminum oxide powder is crucial for assessing its suitability in the production of ceramic parts [19,20]. The bi-modal distribution is often desired, as it allows for increased powder content [21] while simultaneously improving the homogeneity, density, and porosity of the final product [22].

To prepare the feedstock, the  $\text{Al}_2\text{O}_3$  powder was mixed with a binder system based on post-industrial waste PVB from extrusion of various security foils for laminated glasses containing corresponding amount (about 20 wt%) of plasticizer, namely triethylene glycol bis(2-ethylhexanoate) (TEG-EH). The density of the used PVB material, including the TEG-EH, was measured using a gas pycnometer in nitrogen with a result of 1.065 g/cm<sup>3</sup> (Quantachrome Ultrapyc 1200e), while its glass transition temperature was determined to be 29 °C via differential scanning calorimetry (DSC Mettler Toledo DSC 1; 10 °C/min in nitrogen atmosphere).

### 2.2. Feedstock and samples preparation

The determination of the critical solid loading was carried out using the mixing torque method with a Brabender W50 plastometer (Germany). The experiment was performed at a temperature of 170 °C and a mixing speed of 150 rpm. Initially, the powder concentration was set at 50 vol%, and after the torque reached a steady state, the value was recorded, and the mixing device was cleaned. Subsequently, the powder concentration was increased by 1 vol% in incremental steps until the mixing torque did not stabilize and started to increase rapidly, indicating the critical solid loading point. To ensure optimal processing properties, the solid loading for the feedstock was set at a value lower than the critical solid loading point by 4 vol%, as recommended in Ref. [23]. Therefore, the feedstock was prepared with a solid loading of 53 vol%, using the same mixing conditions employed for the determination of the critical solid loading.

In this study, both piston and screw-based injection molding machines were utilized to fabricate CIM samples. The Babyplast 6/10 P-CE injection molding machine (Italy) was employed to manufacture simple round-shaped samples, as shown in Fig. 3a, that are in accordance with the fundamental specifications of CIM technology [24,25]. These samples underwent subsequent debinding and sintering testing. Additionally, the Arburg Allrounder 370S injection molding machine (Germany) was utilized to produce test samples for the three-point bending test, with dimensions of 117 × 12 × 5 before sintering (Fig. 3b).

Table 1 presents the optimized injection molding parameters utilized in this study, which were arrived at through systematic evaluation and adjustment. The selection of these parameters was aimed at attaining the desired characteristics and performance of the fabricated samples, including consistent geometry, dimensional accuracy, and structural integrity. The optimized parameters serve as a basis for further investigations aimed at improving the efficiency and reliability of the injection molding process for CIM applications.

### 2.3. Rheological investigation

An investigation of the rheological properties of feedstock was conducted using a Goettfert RHEO-GRAPH 50 capillary rheometer

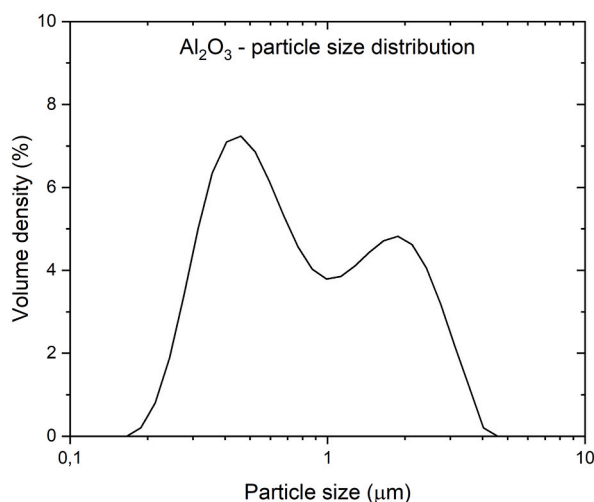
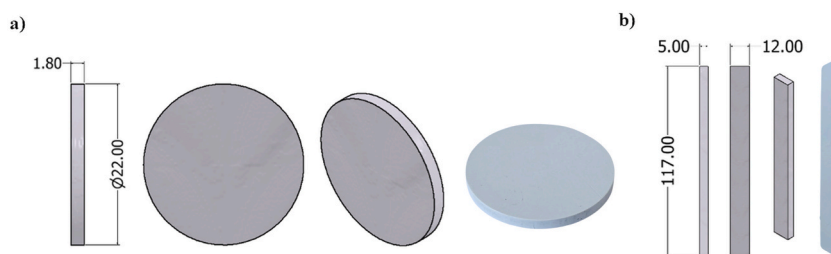


Fig. 2. Particle size distribution curve of  $\text{Al}_2\text{O}_3$  powder.



**Fig. 3.** Shape of testing samples for injection molding, debinding, and sintering processes (a) and for three-point bending test (b), including real injected samples photo.

**Table 1**  
Optimized injection molding parameters.

Injection molding machine	Babyplast 6/10P-CE	Arburg Allrounder 370S
Temperature – zone 1	180 (°C)	160 (°C)
Temperature – zone 2	190 (°C)	170 (°C)
Temperature – zone 3	–	185 (°C)
Temperature – zone 4	–	190 (°C)
Temperature – nozzle	200 (°C)	200 (°C)
Temperature – mold	30 (°C)	30 (°C)
Injection speed	100 (%)	250 (mm/s)
Injection pressure	132 (bar)	2500 (bar)
Hold pressure/time	100/3.5 (bar/s)	2000/5.0 (bar/s)

(Germany) fitted with a 90° entrance angle conical capillary of size 5/0.5 (in mm) at temperatures of 170, 180, and 190 °C. As emphasized in a previous studies [20,26], conical capillaries are essential for accurately measuring highly filled polymers. The commonly used flat capillaries with a 180° entrance angle typically yield overstated rheological values because of the sharp edge at the entrance that does not correspond to the geometrical requirements during the CIM process.

#### 2.4. Debinding and sintering

In this study, the thermal gravimetric analysis of PVB was utilized to establish the most effective debinding process (TGA TA Instruments Q500 Germany; measuring conditions: 600 °C, 5 °C/min, air). The heating ramp must be adjusted according to the sample's thickness, with a low heating ramp of 0.1 °C/min required for samples with a thickness of several millimeters, and a heating ramp of up to 5 °C/min for the smallest samples.

The sintering temperature of the Al<sub>2</sub>O<sub>3</sub> sample was determined using the Hesse Instruments EM301 heating microscope (Germany). The sample was gradually heated to 1650 °C while changes in dimensions and shape were observed to evaluate the sintering temperature. Based on these results, the injected samples were sintered with a 5-h hold in an air atmosphere furnace (Classic 1018S, Czech Republic).

#### 2.5. Density measurement and mechanical testing

The density of the sintered alumina samples was measured using an UltraFoam 1200e Automatic Gas Pycnometer under nitrogen gas (Quantachrome Instruments, USA). Each sintering temperature was tested with 10 replicates.

Flexural properties were investigated using a universal tensile testing machine, specifically the M350-5 CT Materials Testing Machine (Testometric Company, UK). The tests were conducted at a crosshead speed of 2 mm/min with a span length of 68 mm. Each sample was tested with 5 replicates.

### 3. Results and discussion

#### 3.1. Critical solid loading

The behavior of the mixing torque during ceramic powder and binder mixing is an important factor to consider for achieving a homogenous mixture for CIM feedstocks. The critical solid loading refers to the point at which the powder particles are packed as tightly as possible, with the binder system filling all the spaces between them. At solid loading levels below the critical point, the mixing torque is generally stable, increasing gradually as the powder concentration in the mixture increases. However, at the critical solid loading point, the torque increases rapidly due to insufficient binder in the mixture, which causes the friction between the powder particles to become unstable during mixing, in addition once the critical solid loading point is reached, the sudden increase in torque

can result in a non-uniform mixture, potentially leading to defects during injection molding [27].

A comprehensive assessment was conducted to evaluate the stability of the mixing torque over time at various levels of solid loading. Fig. 4 presents representative curves depicting the mixing torque behavior for solid loadings of 50 %, 55 %, and 57 %. Analysis of the results reveals that the torque remains relatively stable up to a solid loading of 57 %. Beyond this point, the torque exhibits signs of instability, indicating the attainment of the critical solid loading.

This critical solid loading value was also confirmed by the behavior of the mixing torque as a function of solid loading, the torque values after stabilization at each solid loading level were plotted in Fig. 5. As can be observed, the mixing torque increased gradually as the solid loading increased. Once the solid loading reached values around 56 vol%, the torque increased rapidly, indicating the critical solid loading for the  $\text{Al}_2\text{O}_3$  feedstock was approximately 56 vol%. The results obtained in this study demonstrate that the critical solid loading point for the industrial waste polymer-based binder system is similar to traditional binder systems based on PVB and PEG (with respect of the type, shape and size of used powder) [28,29]. Therefore, the use of industrial waste polymer did not negatively affect the behavior of the resulting feedstock during mixing, and a stable torque was achieved.

### 3.2. Rheology

Rheological characterization plays a crucial role in the development of highly filled polymers as it provides valuable information on the flow behavior of materials and aids in estimating processing conditions for practical applications [30]. An in-depth comprehension of the rheological properties of such polymeric materials is essential in formulating and processing them effectively. This necessitates a comprehensive understanding of the key factors that affect the rheological behavior of these composites. One crucial factor is the size distribution of the particles, which can significantly affect the rheological behavior of the composites. The shape of the particles are other important considerations that need to be taken into account while analyzing the rheological behavior of highly filled polymers [20,31]. Due to these requirements, the alumina powder used in this study had been previously evaluated in several researchers. The powder possesses favorable specifications and properties, rendering it suitable for use in CIM feedstocks [16,32,33].

Moreover, the rheological behavior of feedstocks is significantly influenced by the interactions between the particles and the matrix, particularly the nature of bonding that occurs between them. In the case of PVB as a binder, its high molecular weight and long-chain structure facilitate strong physical entanglements between the polymer chains and ceramic particles. As a consequence, these entanglements contribute to enhanced interfacial interactions and improved adhesion between the binder and ceramic particles.

Furthermore, the commercial production of PVB involves an acid-catalyzed condensation reaction between butyraldehyde and polyvinyl alcohol (PVA), which is typically hydrolyzed to a large extent. As a result, the resulting polymer is a terpolymer comprising PVB, PVA, and polyvinyl acetate (PVAc) due to incomplete conversion. The presence of residual hydroxyl and acetate groups in the polymer structure can facilitate the adhesion of the PVB to ceramic surfaces. These functional groups may positively influence the bonding between the polymer and ceramic particles, thereby affecting the mechanical properties of the composite material prior to the sintering process [34,35].

Finally, the viscosity of the matrix material itself is another crucial factor that significantly affects the rheological behavior of the highly filled polymers. Polyvinyl butyral (PVB) is a widely used binder in ceramic injection molding (CIM) and has been evaluated in previous studies, often in combination with polyethylene glycol (PEG), to achieve appropriate viscosity values for CIM feedstocks [16, 36]. However, in this study, the use of PEG was replaced with TEG-EH that were sourced from industrial waste polymer. The used plasticizer derived from industrial waste polymer serve as an alternative to PEG and offer several benefits - the use of post-processing scrap as a source of plasticizer contributes to waste reduction, promoting a more sustainable and environmentally responsible manufacturing process.

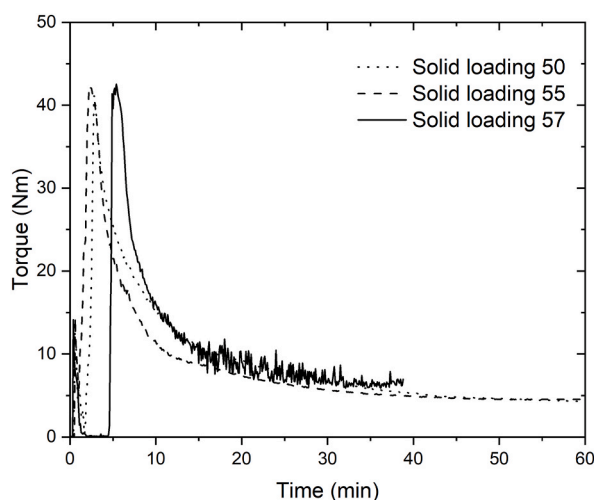


Fig. 4. Mixing torque vs time at different solid loadings.

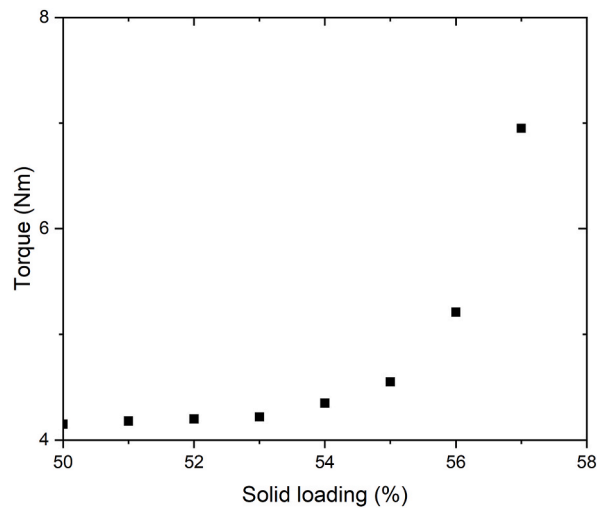


Fig. 5. Mixing torque after stabilization at different solid loadings.

In the literature, it is commonly reported that a viscosity lower than 1000 Pa s is suitable for ceramic injection molding (CIM) feedstocks under the shear rate conditions typically encountered during injection molding [23]. However, the specific viscosity requirements may vary depending on the particular application and the desired properties and shape of the final product. Therefore, rheological characterization of the feedstocks is necessary to determine the appropriate viscosity for each individual case. Generally, the viscosity of CIM feedstocks should be low enough to allow for easy injection of the feedstock into the mold cavity, but high enough to prevent the particles from separation during injection molding.

The viscosity data for the newly developed feedstocks are presented in Fig. 6. The results show that the viscosity values remain below the recommended threshold of 1000 Pa s at shear rates exceeding 1000  $s^{-1}$  [23]. These findings are consistent with the requirements of the CIM process, where shear rates during injection molding typically range in the thousands  $s^{-1}$ . Similar viscosity levels were reported by Medesi [16] for traditional binder systems based on PVB/PEG.

Additionally, Fig. 6 highlights the pseudoplastic behavior of the feedstocks, with viscosity decreasing as shear rate increases. This characteristic is particularly advantageous for injection molding, as it enhances the flow behavior of the feedstocks within the mold cavity. Overall, the viscosity data and observed pseudoplastic behavior of the new binder system indicate that it is suitable for use in CIM technology from a viscosity perspective.

In addition to viscosity, another crucial parameter for assessing the suitability of a feedstock is the flow activation energy (E). The flow activation energy provides insights into the temperature sensitivity of the feedstock. The flow activation energy can be influenced by several factors, including the composition and properties of the binders and powders used in the feedstock formulation. A higher value of flow activation energy indicates that the feedstock is more responsive to temperature variations [37].

Understanding the flow activation energy is crucial because it highlights the temperature conditions that can significantly influence the flow behavior of the feedstock. In ceramic injection molding, precise control of temperature parameters such as injection

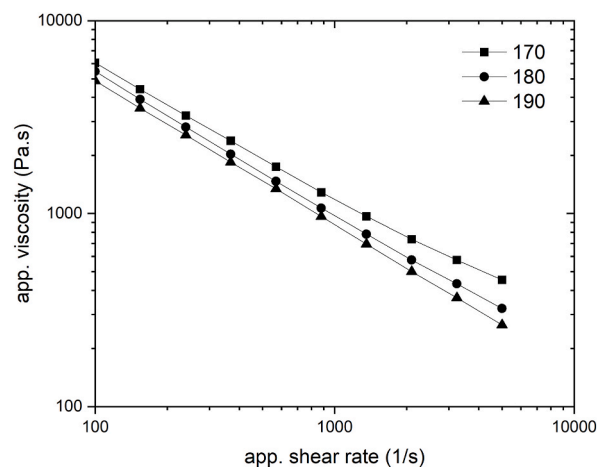


Fig. 6. Relationship between viscosity and shear rate for recycled polymer based feedstock.

temperature and mold temperature is vital. Variations in these temperatures can have a direct impact on the viscosity, flowability, and overall processability of the feedstock. Therefore, it is imperative to carefully monitor and control temperature conditions during the injection molding process, especially when dealing with feedstocks that exhibit high flow activation energy values. Accurate temperature control ensures that the feedstock maintains its desired rheological properties, allowing for successful and consistent molding operations [38].

The activation energy of our feedstock was observed to exhibit a shear-dependent behavior, with an increase observed at higher shear rates (Fig. 7). At low shear rates, the activation energy ranged around 18 kJ/mol, whereas at high shear rates, it reached up to 45 kJ/mol. Similar results of activation energy were obtained by Yan et al. [39] or by Hayat et al. [40], who tested feedstocks based on PEG. Yang et al. reported 50 kJ/mol activation energy at a shear rate  $300 \text{ s}^{-1}$ , where the dependence in this study is not strong, while Hayat et al. did not report the shear rate at which the activation energy was obtained. These findings suggest that when optimizing the injection process, it is advantageous to minimize the injection speed and pressure. This approach helps to reduce the temperature sensitivity of the feedstock, leading to improved process control and stability.

### 3.3. Debinding and sintering

Based on the thermogravimetric analysis (TGA) results presented in Fig. 8, the thermal decomposition behavior of the polyvinyl butyral (PVB) binder system can be characterized by a three decomposition steps. The initial decomposition stage, occurring from approximately  $50 \text{ }^{\circ}\text{C}$ – $330 \text{ }^{\circ}\text{C}$ , accounted for the decomposition of around 25 wt% of the material. This decomposition step primarily involved the degradation of TEG-EH and hydroxyl groups present in the PVB. Subsequently, the second decomposition step took place between  $330 \text{ }^{\circ}\text{C}$  and  $400 \text{ }^{\circ}\text{C}$ , during which approximately 85 % of the polymer underwent degradation. This stage is attributed to the degradation of side groups and main chain scission within the PVB polymer structure. Finally, as the temperature increased beyond  $400 \text{ }^{\circ}\text{C}$ , the decomposition process led usually to the formation of cyclic compounds and oxidation of the carbon residue [41–43].

The thermal debinding process was conducted based on thermogravimetric analysis (TGA) results, employing a series of four distinct holding temperatures:  $150 \text{ }^{\circ}\text{C}$ ,  $250 \text{ }^{\circ}\text{C}$ ,  $350 \text{ }^{\circ}\text{C}$ , and  $450 \text{ }^{\circ}\text{C}$ , with a 2-h holding time. The initial holding temperature of  $150 \text{ }^{\circ}\text{C}$  was carefully selected to ensure the effective decomposition of TEG-EH in the binder system, enabling the removal of the plasticizer without causing damage or deformation to the entire sample. The subsequent holding temperatures were selected to target the decomposition of different chemical groups within the polyvinyl butyral (PVB) binder, as described previously. It is crucial to adhere to these prescribed holding temperatures during the debinding process. Failure to meet these temperature requirements can result in sample deformation, primarily caused by the incomplete degradation of certain components of the binder system prior to further temperature elevation. Therefore, it is imperative to ensure the complete removal of specific binder chemical groups at each step of the debinding process to ensure the preservation of the sample's shape stability [44]. The heating rate employed during the debinding process is another crucial factor that warrants careful consideration. The selection of an appropriate heating rate is typically influenced by the size and thickness of the sample. It is important to strike a balance between the desired debinding efficiency and the prevention of surface deformation. A high heating rate may lead to surface deformation of the sample due to insufficient time for the creation of pores between the ceramic particles, which are necessary for the uniform release of evolving gases. Conversely, employing a lower heating rate allows for a more gradual release of gases and facilitates the formation of evenly distributed pores, thereby minimizing the risk of surface deformation. The controlled evolution of gases and the creation of well-defined pores are crucial for achieving uniform debinding throughout the sample [5,16]. For round shape samples (thickness 1.8 mm) the heating rate of  $3 \text{ }^{\circ}\text{C}/\text{min}$  was optimal, on the other hand, the samples with a higher thickness 5 mm intended for bending tests must be debinded by lower heating rate  $0.1 \text{ }^{\circ}\text{C}/\text{min}$ , when higher heating rate was set up the samples exhibited surface deformation and cracks. Therefore the heating rate should be optimized in each production individually according to sample dimension, the same conclusion were found in previous studies dealing with debinding of highly filled materials [45,46].

Green strength on the injected samples was measured using three-point bending. The results demonstrate that a higher TEG-EH

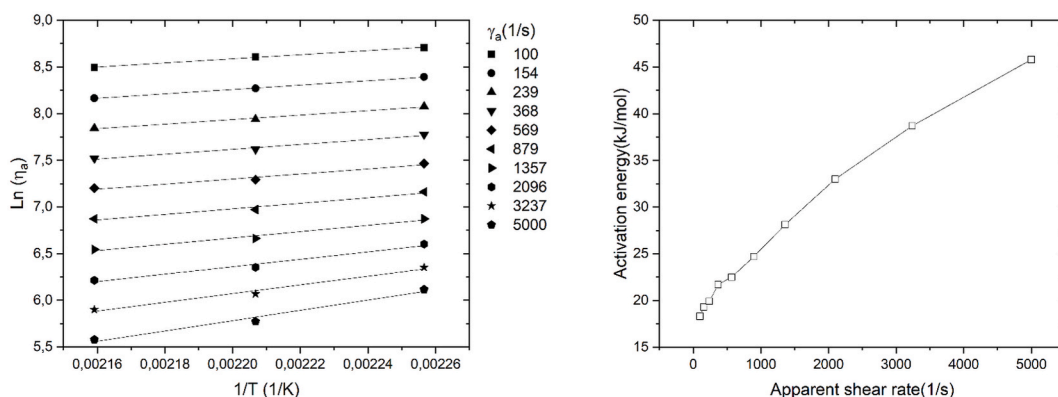


Fig. 7. Flow activation energy represented as the slopes of linear fit for PVB feedstock.

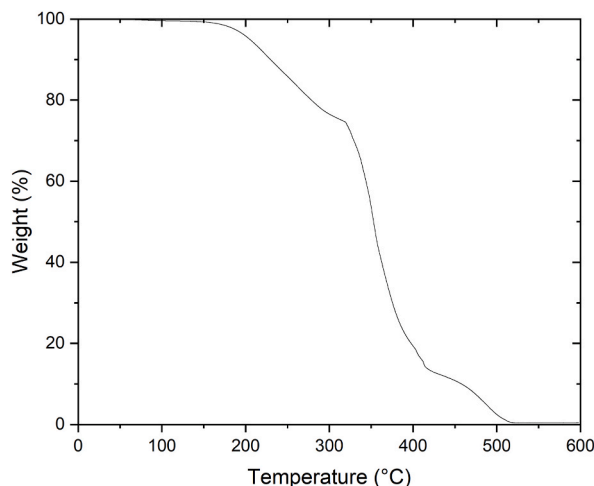


Fig. 8. TGA curve of PVB based binder system.

content significantly influences the mechanical properties of the green injected parts. While the bending strength is lower ( $8.2 \pm 0.2$  MPa) compared to traditional binder systems, which typically exceed 10 MPa, the increased elasticity from the plasticizer compensates for this by making the parts more flexible and less fragile. The increased elasticity is evident in the extended linear elasticity region beyond the 15 mm mark (Fig. 9), which is uncommon in conventional systems. This flexibility makes the parts more resistant to damage during intermediate stages of the CIM process, particularly before sintering. Although the strength is lower, the reduced fragility can be advantageous for handling and transportation [47,48].

A heating microscope was employed to determine the sintering temperature by gradually heating a pressed  $\text{Al}_2\text{O}_3$  powder sample with a standardized height while measuring its dimensional changes. As the temperature increased, the sample's height began to decrease, indicating the onset of sintering due to particle bonding. Through this heating microscopy procedure, it was observed that the sintering process for the  $\text{Al}_2\text{O}_3$  samples initiated at approximately 1300 °C (Fig. 10). According to this finding, a series of sintering experiments was conducted at various temperatures (5 h holding), specifically 1350 °C, 1400 °C, 1450 °C, and 1500 °C. The objective was to investigate the influence of sintering temperature on the final density and mechanical properties of the ceramic samples.

Table 2 presents a comprehensive summary of the influence of varying sintering temperatures on the final density of the products. Notably, the outcomes reveal a direct relationship between sintering temperature and the achieved final product density. Among the investigated sintering temperatures, the highest value, 1500 °C, corresponds to the most substantial density attainment. Specifically, this sintering temperature yielded a relative density of 99.0 % in relation to the pycnometric density ( $4.15 \text{ g/cm}^3$ ). In comparison, the sintering temperature of 1350 °C resulted in a relative density of 95.9 %. The application of high sintering temperatures facilitates the attainment of heightened material densification. Consequently, the progressive elevation of the sintering temperature within the range of 1350–1500 °C improving thermal diffusion rate. As a direct consequence, the sintering kinetics are accelerated, leading to highest material densification. This is in agreement with a similar studies reported in the literature [49,50].

In connection with the density, its higher value also leads to better mechanical properties (Table 3) of the product due to the removal of porosity and increase in intergranular bonding [51].

Firstly, the significant percentual increase in bending modulus from 1350 °C to 1400 °C suggests that this temperature range plays a crucial role in enhancing the stiffness and mechanical strength of the ceramic material. This substantial increase may be attributed to enhanced densification and grain growth within the ceramic matrix [52]. However, as the sintering temperature further increases from 1400 °C to 1450 °C and 1500 °C, the percentual increase in bending modulus becomes less pronounced. This diminishing rate of improvement suggests that beyond a certain point, additional increases in sintering temperature may yield diminishing returns in terms of mechanical property enhancement. This phenomenon could be attributed to the onset of grain coarsening and the emergence of other microstructural defects at higher temperatures, which may offset the benefits of increased densification [53].

Conversely, the percentual increase in bending strength exhibits a consistent upward trajectory with ascending sintering temperatures. Despite observing negligible change in bending strength from 1350 °C to 1400 °C, noteworthy increments are discerned at higher temperatures. Specifically, the bending strength ascends to  $132 \text{ N/mm}^2$  at 1450 °C and further to  $139 \text{ N/mm}^2$  at 1500 °C. This consistent rise in bending strength with increasing sintering temperature suggests a direct correlation between temperature and mechanical properties. As the temperature increases, the material increases its density, reducing the porosity, and enhanced interparticle bonding, leading to improved mechanical strength. The substantial increase in bending strength from 1400 °C to 1500 °C indicates a significant enhancement in the material's ability to resist deformation under applied loads, highlighting the importance of optimizing sintering parameters for achieving superior mechanical properties in ceramic components.

In general, there is a direct and positive relationship between density and mechanical properties in ceramics, including bending modulus. As the density of a ceramic material increases, it typically becomes denser and more closely packed. This results in improved mechanical properties, including increased stiffness (bending modulus) and strength. This relationship is primarily because a denser



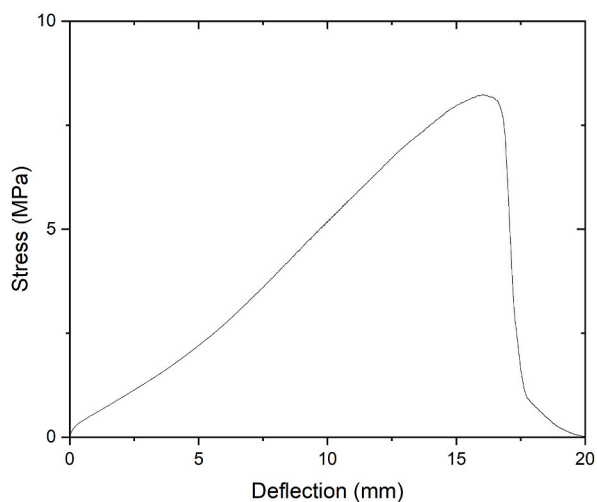


Fig. 9. Three-point bending stress-deflection curves of green injected samples.

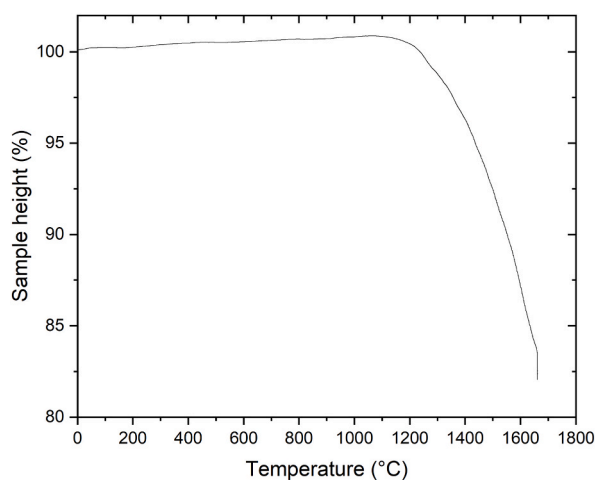


Fig. 10. Heating microscopy analysis of  $\text{Al}_2\text{O}_3$ .

**Table 2**

Density of the final products according the sintering temperature.

Material	Density ( $\text{g}/\text{cm}^3$ )	Relative density (%)
Sintered at 1350 °C	3.98	95,9
Sintered at 1400 °C	4.05	97,6
Sintered at 1450 °C	4.10	98,8
Sintered at 1500 °C	4.11	99,0

**Table 3**

Mechanical properties of the final products according the sintering temperature.

Sintering temperatures (°C)	Bending Modulus ( $\text{N}/\text{mm}^2$ )	Bending Strength ( $\text{N}/\text{mm}^2$ )
1350	$11427 \pm 115$	$125 \pm 3$
1400	$14693 \pm 70$	$124 \pm 2$
1450	$15007 \pm 98$	$132 \pm 2$
1500	$15021 \pm 84$	$139 \pm 3$

material has fewer defects, such as porosity, which can act as stress concentrators and weaken the material [54]. Hence, it can be concluded that a sintering temperature of 1450 °C is adequately sufficient to achieve the high sintered density and optimal mechanical properties. Subsequent increases in sintering temperature result in only marginal enhancements in the final properties of the samples. However, it is noteworthy that pure dense alumina typically exhibits bending strength values ranging between 400 and 450 MPa. Nonetheless, several studies evaluating sintered alumina have reported values significantly lower than this range [55,56]. This discrepancy can be attributed to factors such as large grain size post-sintering, variations in particle size distribution, or failure to achieve 100 % relative density.

#### 4. Conclusions

This study investigated the feasibility of using industrial waste polyvinyl butyral as a binder system for ceramic injection molding and demonstrated its potential as a sustainable alternative to conventional binder systems. The presence of plasticizer in the industrial waste polyvinyl butyral contributed to improved flow properties during the injection molding process. The critical solid loading point was determined at 56 vol%, and rheological testing revealed that the feedstocks had viscosities below 1000 Pa s at shear rates exceeding 1000 s<sup>-1</sup>, which is within the recommended range for ceramic injection molding. The activation energy of the binder system, ranging between 18 kJ/mol and 45 kJ/mol, indicated suitable temperature sensitivity for the injection molding process. Mechanical testing of the sintered ceramic parts yielded favorable results, with final density reaching 4.11 g/cm<sup>3</sup>, a bending modulus of approximately 15000 N/mm<sup>2</sup>, and bending strength reaching up to 139 N/mm<sup>2</sup> at 1500 °C sintering temperature. These properties were comparable to those achieved using traditional binder systems. Therefore, this study confirms that the use of polyvinyl butyral industrial waste not only provides an eco-friendly and cost-effective alternative but also maintains the mechanical and processing properties required for high-quality ceramic injection molding products. This research contributes to the development of sustainable binder systems, supporting broader efforts toward environmental conservation and resource efficiency in the manufacturing industry.

#### CRedit authorship contribution statement

**Daniel Sanetnik:** Writing – original draft, Visualization, Methodology, Investigation, Formal analysis, Data curation, Conceptualization. **Tomas Sedlacek:** Writing – review & editing, Supervision, Conceptualization.

#### Data availability

Data will be made available on request.

#### Declaration of competing interest

The authors declare that they have no known competing financial interests or personal relationships that could have appeared to influence the work reported in this paper.

#### Acknowledgments

This work was supported by the Ministry of Education, Youth and Sports of the Czech Republic – DKRVO (RP/CPS/2024-28/003).

#### References

- [1] R. German, A. Bose. Injection molding of metals and ceramics, Metal Powder Industries Federation, Princeton, New Jersey, 1997, pp. 11–24.
- [2] V.M. Kryachek, Injection moulding (review), powder, Metall. Met. Ceram. 43 (2004) 336–348.
- [3] L. Moballeggh, J. Morshedian, M. Esfandeh, Copper injection molding using a thermoplastic binder based on paraffin wax, Mater. Lett. 59 (2005) 2832–2837.
- [4] T. Jardiel, M.E. Sotomayor, B. Levenfeld, A. Varez, Optimization of the processing of 8-YSZ powder by powder injection molding for SOFC electrolytes, Int. J. Appl. Ceram. 5 (2008) 574–581.
- [5] P. Thomas-Vielma, A. Cervera, B. Levenfeld, A. Varez, Production of alumina parts by powder injection molding with a binder system based on high density polyethylene, J. Eur. Ceram. Soc. 28 (2008) 763–771.
- [6] D. Bleyan, P. Svoboda, B. Hausnerova, Specific interactions of low molecular weight analogues of carnauba wax and polyethylene glycol binders of ceramic injection moulding feedstocks, Ceram. Int. 41 (2015) 3975–3982.
- [7] B. Hausnerova, M. Novak, Environmentally efficient 316L stainless steel feedstocks for powder injection molding, Polymers 12 (2020) 1296.
- [8] J. Wen, Z. Xie, W. Cao, X. Yang, Effects of different backbone binders on the characteristics of zirconia parts using wax-based binder system via ceramic injection molding, J. Adv. Ceram. 5 (2016) 321–328.
- [9] H.w. Li, Y.p. Zhao, G.q. Chen, M.h. Li, X.s. Fu, W.l. Zhou, Synergy of low-and high-density polyethylene in a binder system for powder injection molding of SiC ceramics, Ceram. Int. 48 (2022) 25513–25520.
- [10] Z.Y. Liu, N.H. Loh, S.B. Tor, K.A. Khor, Y. Murakoshi, R. Maeda, Binder system for micropowder injection molding, Mater. Lett. 48 (2001) 31–38.
- [11] G. Thavanayagam, J.E. Swan, Aqueous debinding of polyvinyl butyral based binder system for titanium metal injection moulding, Powder Technol. 326 (2018) 402–410.
- [12] M. Song, M. Park, J. Kim, I. Cho, K. Kim, H. Sung, S. Ahn, Water-soluble binder with high flexural modulus for powder injection molding, J. Mater. Sci. 40 (2005) 1105–1109.
- [13] H.I. Bakan, Injection moulding of alumina with partially water soluble binder system and solvent debinding kinetics, Mater. Sci. Technol. 23 (2007) 787–791.
- [14] M.D. Hayat, T. Li, G. Wen, P. Cao, Suitability of PEG/PMMA-based metal injection moulding feedstock: an experimental study, Int. J. Adv. Manuf. Technol. 80 (2015) 1665–1671.

- [15] M.D. Hayat, H. Zhang, K.M. Karumbaiah, H. Singh, Y. Xu, L. Zou, X. Qu, S. Ray, P. Cao, A novel PEG/PMMA based binder composition for void-free metal injection moulding of Ti components, *Powder Technol.* 382 (2021) 431–440.
- [16] A.J. Medesi, D. Notzel, T. Hanemann, PVB/PEG-Based feedstocks for injection molding of alumina microreactor components, *Materials* 12 (2019) 1219.
- [17] Y. Thomas, B.R. Marple, Partially water-soluble binder formulation for injection molding submicrometer zirconia, *Adv. Perform. Mater.* 5 (1998) 25–41.
- [18] A.R. Tripathy, W. Chen, S.N. Kukureka, W.J. MacKnight, Novel poly(butylene terephthalate)/poly(vinyl butyral) blends prepared by in situ polymerization of cyclic poly(butylene terephthalate) oligomers, *Polymers* 44 (2003) 1835–1842.
- [19] B. Hausnerova, T. Kitano, I. Kuritka, J. Prindis, L. Marcanikova, The role of powder particle size distribution in the processability of powder injection molding compounds, *Int. J. Polym. Anal. Char.* 16 (2011) 141–151.
- [20] D. Sanetnik, B. Hausnerova, M. Novak, B.N. Mukund, Effect of particle size and shape on wall slip of highly filled powder feedstocks for material extrusion and powder injection molding, *3D Print. Addit. Manuf.* 10 (2023) 236–244.
- [21] A.V. Mityukov, V.A. Govorov, A.Y. Malkin, V.G. Kulichikhin, Rheology of highly concentrated suspensions with a bimodal size distribution of solid particles for powder injection molding, *Polymers* 13 (2021) 2709.
- [22] B.N. Mukund, B. Hausnerova, T.S. Shivashankar, Development of 17-4PH stainless steel bimodal powder injection molding feedstock with the help of interparticle spacing/lubricating liquid concept, *Powder Technol.* 283 (2015) 24–31.
- [23] R.M. German, *Metal Injection Molding*, Metal Powder Industries Federation, Princeton, New Jersey, 2011.
- [24] B. Hausnerova, D. Sanetnik, P. Ponizil, Surface structure analysis of injection molded highly filled polymer melts, *Polym. Compos.* 34 (2013) 1553–1558.
- [25] P.J. Vervoort, R. Vetter, J. Duszczak, Overview of powder injection molding, *Adv. Perform. Mater.* 3 (1996) 121–151.
- [26] D. Sanetnik, B. Hausnerova, P. Filip, E. Hnatková, Influence of capillary die geometry on wall slip of highly filled powder injection molding compounds, *Powder Technol.* 325 (2018) 615–619.
- [27] D. Lin, D. Sanetnik, H. Cho, S.T. Chung, Y.S. Kwon, K.H. Kate, B. Hausnerova, S.V. Atre, S.J. Park, Rheological and thermal debinding properties of blended elemental Ti-6Al-4V powder injection molding feedstock, *Powder Technol.* 311 (2017) 357–363.
- [28] D. Nötzel, T. Hanemann, New feedstock system for fused filament fabrication of sintered alumina parts, *Materials* 13 (2020) 4461.
- [29] E. Hnatkova, B. Hausnerova, P. Filip, Evaluation of powder loading and flow properties of Al<sub>2</sub>O<sub>3</sub> ceramic injection molding feedstocks treated with stearic acid, *Ceram. Int.* 45 (2019) 20084–20090.
- [30] I. Duretek, C. Holzer, Material flow data for numerical simulation of powder injection molding, *Univers. J. Mater. Sci.* 5 (2017) 7–14.
- [31] B. Hausnerova, B.N. Mukund, D. Sanetnik, Rheological properties of gas and water atomized 17-4PH stainless steel MIM feedstocks: effect of powder shape and size, *Powder Technol.* 312 (2017) 152–158.
- [32] B. Hausnerova, L. Marcanikova, P. Filip, P. Saha, Rheological characterization of powder injection moulding using feedstock based on aluminium oxide and multicomponent water-soluble polymer binder, *Recent Adv. Fluid Mech. Heat Mass Transfer* (2011) 245–250.
- [33] B. Hausnerova, D. Sanetnik, V. Pata, Surface properties of powder injection moulded parts related to processing conditions, *Manuf. Technol.* 18 (2018) 895–899.
- [34] Y. Wang, X. Li, R. Liang, H. Zhu, H. Wu, F. Liu, Y. Liu, F. Niu, Effects of PVB addition on PbO ceramics used in lead-cooled fast reactors, *Prog. Nucl. Energy* 151 (2022) 104346.
- [35] W. Liu, W. Zhang, J. Li, D. Zhang, Y. Pan, Preparation of spray-dried powders leading to Nd:YAG ceramics: the effect of PVB adhesive, *Ceram. Int.* 38 (2012) 259–264.
- [36] T. Kosalwit, P. Pakunthod, W. Pinthong, P. Sooksaeen, N. Chuankrerkkul, Powder injection moulding of alumina using PEG/PVB binder systems, *Key Eng. Mater.* 545 (2013) 173–176.
- [37] A.V. Shenoy, *Rheology of Filled Polymer Systems*, Springer, 1999.
- [38] D.F. Heaney, *Handbook of Metal Injection Molding*, Woodhead Publishing, Duxford, United Kingdom, 2019.
- [39] W. Yang, K. Yang, M. Hon, Effects of PEG molecular weights on rheological behavior of alumina injection molding feedstocks, *Mater. Chem. Phys.* 78 (2003) 416–424.
- [40] M.D. Hayat, G. Wen, M.F. Zulkifli, P. Cao, Effect of PEG molecular weight on rheological properties of Ti-MIM feedstocks and water debinding behaviour, *Powder Technol.* 270 (2015) 296–301.
- [41] L.C.K. Liao, T.C.K. Yang, D.S. Viswanath, Mechanism of degradation of poly(vinyl butyral) using thermogravimetry/fourier transform infrared spectrometry, *Polym. Eng. Sci.* 36 (1996) 2589–2600.
- [42] J.J. Seo, S.T. Kuk, K. Kim, Thermal decomposition of PVB (polyvinyl butyral) binder in the matrix and electrolyte of molten carbonate fuel cells, *J. Power Sources* 69 (1997) 61–68.
- [43] A.K. Dhaliwal, J.N. Hay, The characterization of polyvinyl butyral by thermal analysis, *Thermochim. Acta* 391 (2002) 245–255.
- [44] E.S. Thian, N.H. Loh, K.A. Khor, S.B. Tor, Effects of debinding parameters on powder injection molded Ti-6Al-4V/HA composite parts, *Adv. Powder Technol.* 12 (2001) 361–370.
- [45] S. Supriadi, E.R. Baek, G. Maulana, R. Hidayatullah, B. Suharno, Thermal debinding process of SS 17-4 PH in metal injection molding process with variation of heating rates, temperatures, and holding times, *Solid State Phenom.* 266 (2017) 238–244.
- [46] J. Gu, L. Qiao, W. Cai, J. Zheng, Y. Ying, J. Yu, W. Li, S. Che, Effects of heating rate in thermal debinding on the microstructure and property of sintered NiCuZn ferrite prepared by powder injection molding, *J. Magn. Magn Mater.* 530 (2021) 167931.
- [47] Q. Mao, L. Qiao, J. Zheng, Y. Ying, J. Yu, W. Li, S. Che, W. Cai, Injection molding and sintering of ZrO<sub>2</sub> ceramic powder modified by a zirconate coupling agent, *Materials* 15 (2022) 7014.
- [48] X. Jiang, D. Li, R. Lu, Z. Yang, Z. Liu, Study of hyperbranched polymer on POM-based binder in metal injection molding, *Mater. Res. Express* 6 (2019) 125377.
- [49] O. Ogunbiyi, S. Salifu, R. Sadiku, T. Jamiru, O. Adesina, O.S. Adesina, Influence of sintering temperature on microstructure and mechanical properties of graphene-reinforced Inconel 738 LC composites, *Mater. Today Proc.* 38 (2021) 743–748.
- [50] A. Oketola, T. Jamiru, A.T. Adegbola, O. Ogunbiyi, R. Sadiku, S. Salifu, Influence of sintering temperature on the microstructure, mechanical and tribological properties of ZrO<sub>2</sub> reinforced spark plasma sintered Ni–Cr, *Int. J. Lightweight Mater. Manuf.* 5 (2022) 188–196.
- [51] D.C. Jana, P. Barick, B.P. Saha, Effect of sintering temperature on density and mechanical properties of solid-state sintered silicon carbide ceramics and evaluation of failure origin, *J. Mater. Eng. Perform.* 27 (2018) 2960–2966.
- [52] T. Yu, Z. Zhao, J. Li, Effect of sintering temperature and sintering additives on the properties of alumina ceramics fabricated by binder jetting, *Ceram. Int.* 49 (2023) 9948–9955.
- [53] Y. Shao, W. Yu, J. Wu, H. Ma, Effect of sintering temperatures on grain coarsening behaviors and mechanical properties of W-NiTi heavy tungsten alloys, *Materials* 15 (2022) 8035.
- [54] A.A. Adam, H.A. Bakar, U.A. Amani, L.H. Pajjan, N.A. Wahab, M.F. Mamat, M.B. Ali, S.G. Herawan, Z. Ahmad, Effect of sintering parameters on the mechanical properties and wear performance of alumina inserts, *Lubricants* 10 (2022) 325.
- [55] J. Vogt, H. Friedrich, M. Stepanyan, C. Eckardt, M. Lam, D. Lau, B. Chen, R. Shan, J. Chan, Improved green and sintered density of alumina parts fabricated by binder jetting and subsequent slurry infiltration, *Prog. Addit. Manuf.* 7 (2022) 161–171.
- [56] J. Kim, J. Ha, J. Lee, I. Song, Optimization for permeability and electrical resistance of porous alumina-based ceramics, *J. Korean Ceram. Soc.* 53 (2016) 548–556.